

# Optimal b-Value Range in Diffusion Kurtosis Imaging

Ezequiel Farher<sup>1</sup>, Farida Grinberg<sup>1</sup>, and N. Jon Shah<sup>1,2</sup>

<sup>1</sup>Institute of Neuroscience and Medicine - 4, Forschungszentrum Juelich, Juelich, Germany, <sup>2</sup>JARA - Faculty of Medicine, RWTH Aachen University, Aachen, Germany

## Introduction

Due to constraints imposed by complex cellular microstructure, molecular propagation of water in biological tissues differs from the Gaussian diffusion profile observed in bulk free water. The deviations become significant at  $b$ -values exceeding the standard range used in DTI, i.e. above  $1000 \text{ s mm}^{-2}$ . Diffusion kurtosis imaging (DKI) was proposed as a model-free approach to quantify these deviations [1]. DKI is applicable only in the moderate range of  $b$ -values below the maximum value,  $b_{\max} = 3/(D_{\text{app}}K_{\text{app}})$ , which corresponds to the minimum of the diffusion attenuation curve. This is an intrinsic limitation of DKI as it predicts, above  $b_{\max}$ , an (unphysical) increase of the signal due to a truncation of the cumulant expansion of the signal logarithm at the second term. Therefore, in human brain tissue DKI analysis is restricted to the typical range of  $(2000 - 3000) \text{ s mm}^{-2}$ . However, due to anisotropy of cellular architecture, both the apparent diffusivity,  $D_{\text{app}}$ , and the apparent excess kurtosis,  $K_{\text{app}}$ , are not isotropic and depend on the direction of diffusion-encoding gradients. Thus,  $b_{\max}$  is also a function of orientation. Moreover, since  $D_{\text{app}}$  and  $K_{\text{app}}$  are different in different tissues,  $b_{\max}$  might be different in different tissues too. Various optimization schemes with respect to  $b$ -value sets were suggested for standard DTI parameters [2] (such as mean diffusivity or fractional anisotropy). In DKI, proposed optimization procedures [3] were rather related to the gradient settings. However, the influence of the  $b$ -value range on the evaluated DKI metrics was not sufficiently investigated. In this work we study the impact of the selected  $b$ -value range on the evaluation of the DKI metrics and propose a simple optimization method which permits one to enhance the accuracy of quantitative parameter estimations.

## Materials and methods

MRI experiments were carried out in a whole-body 3T Siemens Trio scanner (Siemens Medical Systems, Erlangen, Germany) with healthy volunteers under ethical approval. A twice-refocused spin-echo sequence with bipolar diffusion gradients was applied using  $b$ -values in the range between 0 and  $7000 \text{ s mm}^{-2}$  and various sets of diffusion gradients. The data were processed and DKI metrics were evaluated as described in Ref. [4] using the kurtosis equation,  $S(b) = \exp\left(-bD_{\text{app}} + \frac{1}{6}(bD_{\text{app}})^2 K_{\text{app}}\right)$ .

In a first step, we quantified the effect of the  $b$ -value range on the mean diffusivity and mean kurtosis for the six ranges of increasing  $b$ -values:  $R_1$ ,  $[0-1500] \text{ s mm}^{-2}$ ;  $R_2$ ,  $[0-2000] \text{ s mm}^{-2}$ ;  $R_3$ ,  $[0-2500] \text{ s mm}^{-2}$ ;  $R_4$ ,  $[0-3000] \text{ s mm}^{-2}$ ;  $R_5$ ,  $[0-3500] \text{ s mm}^{-2}$ ;  $R_6$ ,  $[0-4000] \text{ s mm}^{-2}$ . Here, we used the largest set of 15  $b$ -values measured with the smallest number of 6 gradient directions to reduce the acquisition time. We evaluated the maps of  $b_{\max}$  on a voxel-by-voxel basis. In each voxel, kurtosis equation was iteratively fitted to the normalized signal-attenuation curves by step-wise increasing the  $b$ -value range, and evaluating  $b_{\max}$  from the fitted values of  $D_{\text{app}}$  and  $K_{\text{app}}$  until the condition  $b < b_{\max}$  was violated for the largest value of the range. For an optimised evaluation of the mean kurtosis maps we then used the  $b$ -value range below  $b_{\max}$  individually in each voxel. A similar procedure was applied to evaluate kurtosis values for different orientation dependent  $b_{\max}$ .

Figure 1a illustrates how the chosen  $b$ -value range affects evaluation of  $K_{\text{app}}$  in both white matter (WM) and non-white matter (non-WM). The data refer to the two selected slices, one containing the CSF ventricle, and the other not. Figure 1a shows that with increasing the range of  $b$ -values, kurtosis values significantly decrease. (The noisy appearance of the map for  $R_1$  is attributed to the fact that the deviations from the Gaussian behaviour in this range are too low for an accurate quantification). The evolution of DKI metrics with increasing the  $b$ -value range is demonstrated quantitatively by the histograms in Figures 1b and 1c (second slice) evaluated for all six  $b$ -value ranges,  $R_i$  ( $i = 1 \dots 6$ ). Whereas the peak of  $D_{\text{app}}$  in Figure 1b is practically independent of  $R_i$ , both peaks in the histograms of  $K_{\text{app}}$  (Figure 1c) tend to significantly shift towards lower values, the larger the  $b$ -value range (see dashed lines visualizing the peak positions beneath the histograms). The peaks are attributed to WM and non-WM [3]. Figure 2 shows the maps of  $b_{\max}$ . It clearly demonstrates that  $b_{\max}$  is inhomogeneous across the brain. The observed patterns are correlated with the contrast patterns of different tissues: WM, non-WM, CSF, and voxel sets contaminated by partial volume effects. Figure 3 shows the maps of  $K_{\text{app}}$  evaluated using the voxel-dependent  $b_{\max}$ . The results are discussed in the context of improving the quantitative analysis of the DKI metrics and reducing their variability in dependence of acquisition parameters.

## Results and discussions

Figure 1a illustrates how the chosen  $b$ -value range affects evaluation of  $K_{\text{app}}$  in both white matter (WM) and non-white matter (non-WM). The data refer to the two selected slices, one containing the CSF ventricle, and the other not. Figure 1a shows that with increasing the range of  $b$ -values, kurtosis values significantly decrease. (The noisy appearance of the map for  $R_1$  is attributed to the fact that the deviations from the Gaussian behaviour in this range are too low for an accurate quantification). The evolution of DKI metrics with increasing the  $b$ -value range is demonstrated quantitatively by the histograms in Figures 1b and 1c (second slice) evaluated for all six  $b$ -value ranges,  $R_i$  ( $i = 1 \dots 6$ ). Whereas the peak of  $D_{\text{app}}$  in Figure 1b is practically independent of  $R_i$ , both peaks in the histograms of  $K_{\text{app}}$  (Figure 1c) tend to significantly shift towards lower values, the larger the  $b$ -value range (see dashed lines visualizing the peak positions beneath the histograms). The peaks are attributed to WM and non-WM [3]. Figure 2 shows the maps of  $b_{\max}$ . It clearly demonstrates that  $b_{\max}$  is inhomogeneous across the brain. The observed patterns are correlated with the contrast patterns of different tissues: WM, non-WM, CSF, and voxel sets contaminated by partial volume effects. Figure 3 shows the maps of  $K_{\text{app}}$  evaluated using the voxel-dependent  $b_{\max}$ . The results are discussed in the context of improving the quantitative analysis of the DKI metrics and reducing their variability in dependence of acquisition parameters.

## Conclusions

We demonstrated that evaluation of DKI metrics strongly depends on the acquisition parameters. Implementation of a voxel-based estimation of  $b_{\max}$  helps to improve the accuracy of evaluation of DKI metrics and reduce its dependence on the selection of specific gradient orientations and  $b$ -value sets. This is especially important when DKI parameters are exploited as biomarkers of neurological pathologies [5,6] or aging effects [7] of human brain tissue. Further development of optimization schemes for both acquisition and postprocessing of DKI is necessary. This kind of work is currently in process in our laboratory.

## References

[1] Jensen, J.H. et al. *Magn Reson Med* **53**, 1432-1440 (2005). [2] Veraa, J. et al. *Magn Reson Med* **65**, 138-145 (2011). [3] Poot, D.H.J. et al. *IEEE T Med Imaging* **29**, 819-829 (2010). [4] Grinberg, F. et al. *Neuroimage* **57**, 1087-1102 (2011). [5] Jensen, J.H. et al. *NMR Biomed* **24**, 452-457 (2011). [6] Grinberg, F. et al. *Proc. Intl. Soc. Mag. Reson. Med.* **19**, 1989 (2011). [7] Falangola, M.F. et al. *J Magn Reson Imaging* **28**, 1345-1350 (2008).

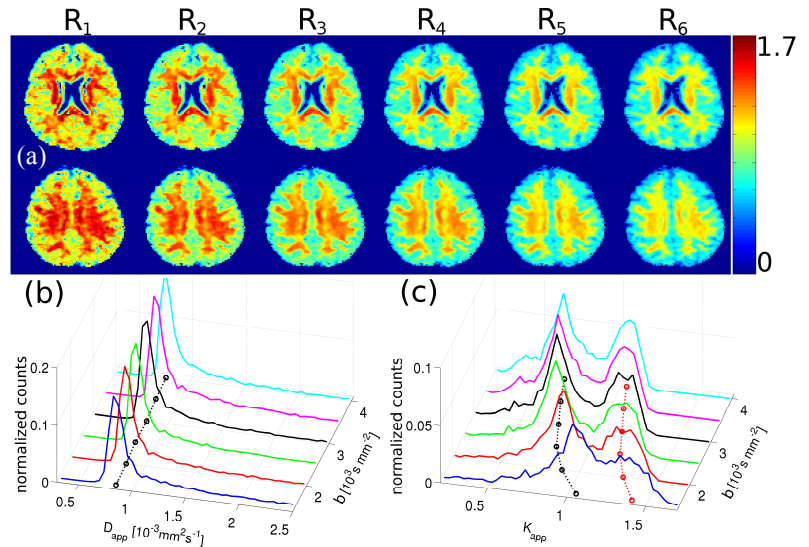


**Figure 1.** (a) dependence of  $K_{\text{app}}$  on the selected range of  $b$ -value,  $R_i$  ( $i = 1 \dots 6$ , from left to right). (b-c) the histograms of  $D_{\text{app}}$  and  $K_{\text{app}}$  for each of the  $b$ -value ranges. The dashed line in the bottom shows the peak of each histogram.

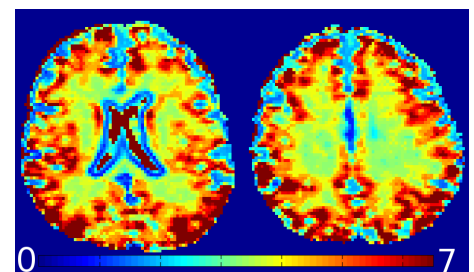


**Figure 2.** The maps of  $b_{\max}$  for the two slices. The units are  $10^3 \text{ s mm}^{-2}$ .

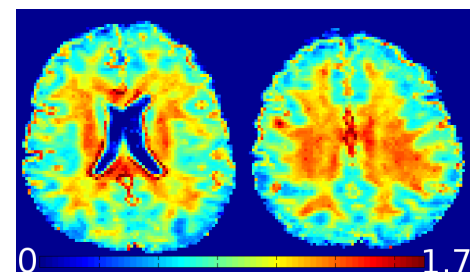


**Figure 3.** The maps of  $K_{\text{app}}$  evaluated iteratively.